Simple mitigation of global depolarizing errors in quantum simulations

Joseph Vovrosh,[1,*] Kiran E. Khosla,[1] Sean Greenaway,[1] Christopher Self,[1] M. S. Kim,[1] and Johannes Knolle[2,3,1]
[1]*Blackett Laboratory, Imperial College London, London SW7 2AZ, United Kingdom*
[2]*Department of Physics TQM, Technische Universität München, James-Franck-Straße 1, D-85748 Garching, Germany*
[3]*Munich Center for Quantum Science and Technology (MCQST), 80799 Munich, Germany*

(Received 9 January 2021; revised 28 April 2021; accepted 3 September 2021; published 30 September 2021)

To get the best possible results from current quantum devices error mitigation is essential. In this work we present a simple but effective error mitigation technique based on the assumption that noise in a deep quantum circuit is well described by global depolarizing error channels. By measuring the errors directly on the device, we use an error model ansatz to infer error-free results from noisy data. We highlight the effectiveness of our mitigation via two examples of recent interest in quantum many-body physics: entanglement measurements and real-time dynamics of confinement in quantum spin chains. Our technique enables us to get quantitative results from the IBM quantum computers showing signatures of confinement, i.e., we are able to extract the meson masses of the confined excitations which were previously out of reach. Additionally, we show the applicability of this mitigation protocol in a wider setting with numerical simulations of more general tasks using a realistic error model. Our protocol is device-independent, simply implementable, and leads to large improvements in results if the global errors are well described by depolarization.

DOI: 10.1103/PhysRevE.104.035309

I. INTRODUCTION

Quantum computers are becoming large enough (∼50–100 qubits [1]) to, in principle, allow demonstrations of their "quantum advantage" [2,3]. However, the actual amount of entanglement that can be generated in current devices is constrained by noise and errors, limiting their ability to solve complex problems such as quantum simulation. To address this, various *error mitigation* strategies have recently been developed to counteract noise and boost the fidelity of experimental results.

Error mitigation differs from fault tolerance. Fault tolerant quantum computers will eventually be able to suppress errors by encoding quantum information in a redundantly large number of qubits as error correcting codes [4,5]. In this way they will be able to execute arbitrarily deep circuits by the repeated application of active error corrections. Unfortunately, these encodings cannot be used in current devices as they require smaller hardware errors and larger numbers of qubits than are currently available. In contrast, error mitigation strategies are applied to unencoded physical qubits. Rather than actively correcting errors, they aim to estimate what the effect of the error was and infer the error-free result. This current stage in the development of quantum computers has been dubbed the noisy intermediate-scale quantum (NISQ) era [1] and is expected to last for the foreseeable future.

In the past few years, error mitigation has been a thriving research direction as more and more quantum devices become available. Error mitigation strategies typically address measurement errors [7–15] or the algorithms and gates employed for digital quantum simulation [16–23]. While some of these techniques have proven useful for certain quantum algorithms, their general success is hampered by the fact that they either rely on a high level of control of the quantum device itself, or are specifically designed for a given quantum simulation problem, i.e., exploiting specific symmetries [24].

One promising direction is to employ machine learning algorithms [25–28] for error mitigation. Generally speaking, these methods train classical computers to predict the error seen in a quantum device and use the results to infer the error-free quantum simulations. While successful, these methods require a large increase in the classical computational overhead and are somewhat uncontrolled. The latter drawback is also true for popular protocols based on the idea of increasing errors in the device systematically and then extrapolating back to the zero error case [21,29–35]. In general, how to tune the error rates varies from device to device and reliable fitting requires expert knowledge of the specific hardware.

Here, we propose a new protocol for gate error mitigation combining a raft of desirable features: It is easily implementable on any quantum device with little increase in workload, it is well rooted in a mathematical description of the errors, and it is suitable for any quantum algorithm of interest. Furthermore, as we show via specific examples, it can lead to large improvements in the performance of quantum devices; for example, see Fig. 1 for Rényi entropy results.

The paper is organized as follows: First, we derive an ansatz for the density matrix resulting from the action of a noisy quantum simulator with global depolarizing errors. Following this, we explain how this ansatz can be used for a general error mitigation protocol. We then demonstrate its effectiveness by studying real time dynamics of the transverse field Ising model (TFIM) with a longitudinal field. In that context, some of the authors recently showed that signatures of confinement and entanglement spreading can be observed

*jwv18@ic.ac.uk

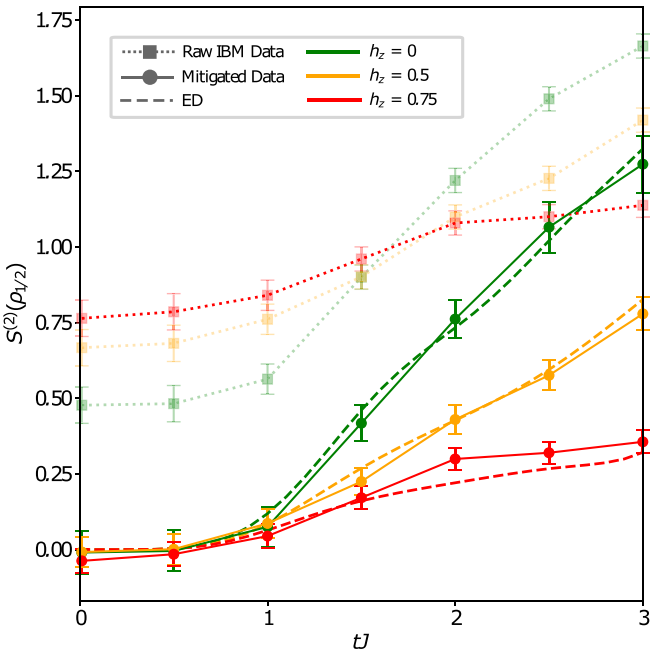

FIG. 1. Results from the IBM device *ibmq_paris* [6] of the second-order Rényi entanglement entropy. Quench dynamics before and after error mitigation of the second-order Réyni entropy for the transverse field Ising model with varying longitudinal field strengths. Here, $J = 1$, $h_x = 0.5$, and $n = 6$. Note, 800 random unitaries were used to collect this data giving an uncertainty in the purity of $\delta\rho \sim O(10^{-2})$. Clearly the mitigation allows results to go from qualitative agreement to quantitative agreement with the results obtained numerically through exact diagonalization (ED).

on an IBM quantum computer [36]. With our new error mitigation protocol we are able to measure the meson masses of confinement induced bound states directly on the IBM device and can quantitatively measure entanglement spreading previously out of reach. Furthermore, we corroborate these results with classical simulations of error models taken from an IBM Quantum device in a more general setting to show the wide applicability of our mitigation scheme. Finally, we close with a discussion and outline future applications.

II. ERROR MITIGATION PROTOCOL

Our error mitigation protocol is based on the assumption that the gate errors that plague a deep quantum circuit are well described by a *global depolarizing* error model. Here we give a heuristic argument to justify this approximation.

Error channels can be conveniently modeled through Kraus operators [37] which define a completely positive map on the density matrix

$$\rho \to \sum_i K_i \rho K_i^\dagger \quad \text{such that} \quad \sum_i K_i^\dagger K_i = 1. \tag{1}$$

For a single qubit, choosing four Kraus operators to be proportional to the Pauli operators (identity included) defines a depolarizing channel. The proportionality constants are related to the individual error probabilities and must satisfy the identity constraint to preserve the trace of ρ.

Here, we concentrate on such depolarizing errors which are inevitably present in any digital quantum simulator platform and can be treated without much specific knowledge about the device performance (which also fluctuates over time). Moreover, our focus on depolarizing errors has the advantage of being treatable mathematically in a controlled way as detailed below. In fact, given a deep enough quantum circuit (with sufficient qubits) for self-averaging of incoherent errors to occur, this depolarizing error model is a good approximation to the physical errors in a device [38]. Last but not least, the large improvement in the quality of results on the IBM device motivate our choice of depolarizing errors *a posteriori*.

An n-single qubit depolarizing error channel can be modeled via

$$\mathcal{E}^{\otimes n}(\rho) = (1-p)^n \rho + \sum_{\alpha\in[x,y,z]} \sum_{j=1}^{n} (1-p)^{n-1} \frac{p}{3} \sigma_\alpha^j \rho \sigma_\alpha^j + ..., \tag{2}$$

where $\mathcal{E}$ is the error channel, p is the probability of an error occurring for each qubit (assumed to be equal for each qubit, and for each Pauli error) and "..." indicates higher-order terms corresponding to errors on multiple qubits [37]. One important feature of this mathematical formulation is that the second term, which describes the depolarizing error, commutes with any unitary operator. Consequently, the error on the ith qubit in a quantum circuit with purely depolarizing errors is

$$\mathcal{E}^i(\rho) = (1-p_i)\rho + p \mathrm{Tr}_i[\rho] \otimes \frac{\mathcal{I}_i}{2}, \tag{3}$$

in which ρ is the density matrix, $\mathcal{I}_i/2$ is the maximally mixed (i.e., completely depolarized) state for the ith qubit, Tr_i is the partial trace over the ith qubit, and p_i is the error on the ith qubit.

Instead of dealing with all combinations of single qubit errors, we approximate the total error channel of Eq. (2), under the assumption of symmetric depolarization Eq. (3), as an effective depolarizing channel on the *entire* quantum state

$$\rho = (1 - p_{\mathrm{tot}})\rho_{\mathrm{exact}} + p_{\mathrm{tot}} \frac{\mathcal{I}^{\otimes n}}{2^n}, \tag{4}$$

where the effective *total* error probability is p_{tot}. In principle, p_{tot} is well approximated by $\prod_i (1 - p_i)$; however, we do not make that identification here. We will soon show that p_{tot} can be measured directly on the device. The simplicity of this ansatz allows it to be easily calculated. It has already been shown to be useful when mitigating measurement error [39]; however, we later demonstrate that it is powerful tool for mitigating global depolarizing errors which do not themselves originate from local depolarizing errors. Furthermore, we later numerically demonstrate that this ansatz does not rely on the assumption of single- and two-qubit depolarizing errors.

The many partial traces over single qubits, which would have conserved some coherence in the remaining qubits, have been replaced by the maximally mixed state $\mathcal{I}^{\otimes n}/2^n$ over the global quantum state, destroying all coherence. We stress that even though this may not be a good approximation for a single layer of qubit errors, it becomes a reasonable approximation for the error channel of a many layer, many qubit circuit. Eq. (4) is our basic ansatz for an effective error model after

a many-layered unitary circuit and ρ_{exact} is the exact density operator without noise.

For a rigorous derivation of the ansatz used in this paper we turn to work done by Zhenyu Cai [34]. In this, the author starts with the assumption that the noise of a quantum device can be well described by a general Pauli noise model. From this, they derive the resulting density matrix, which they present as a series expansion. The global depolarizing ansatz used in our work is a special case of the leading order term in this expansion.

With this ansatz one can analytically calculate the effect of errors on a measured observable, $\hat{O}$, via

$$\langle\hat{O}\rangle = (1 - p_{\text{tot}})\text{Tr}[\hat{\text{O}}\rho_{\text{exact}}] + \frac{\text{p}_{\text{tot}}}{2^{\text{n}}}\text{Tr}[\hat{\text{O}}]. \tag{5}$$

Our approach estimates p_{tot} to apply error mitigation. We propose and test two approaches for finding p_{tot}, the first based on estimating the purity of the final state and the second based on studying specific observables. To estimate the purity, we employ the recent protocol for obtaining the trace of the reduced density matrix squared $\text{Tr}[\rho_{\text{A}}^2]$ via randomized measurements [40,41], where A is a subspace of the full density matrix. This randomized measurement scheme has been successfully implemented in trapped ion quantum simulators [42] and recently by some of us on an IBM quantum computer [36]. We stress the present mitigation is a far simpler task compared to inverting the quantum error channel to tomographically reconstruct the error free quantum state ρ.

As current quantum devices initialize systems in pure states that are then manipulated with unitary transformations, $\text{Tr}[\rho^2]$ over the full Hilbert space should lead to a result that is identically one. However, since the noisy implementation of quantum circuits will in general deviate from unitarity, after a given quantum circuit is run on a quantum processor this will generally not be the case. Instead, with Eq. (4) we expect that

$$\text{Tr}[\rho^2] = (1 - \text{p}_{\text{tot}})^2 + \frac{\text{p}_{\text{tot}}(1 - \text{p}_{\text{tot}})}{2^{\text{n}-1}} + \frac{\text{p}_{\text{tot}}^2}{2^{\text{n}}}. \tag{6}$$

Using the fact that ρ_{exact} is pure. Now, given that the left-hand side, $\text{Tr}[\rho^2]$, can be measured directly on the device [36,42], this quadratic equation can be solved to obtain the total error p_{tot} [39,43]. We stress that correlated errors in quantum circuits do not increase entropy and thus p_{tot} obtained via this method should really be understood as the *global depolarizing* error probability. While this mitigation approach does not address coherent errors, it could additionally be combined with other techniques such as twirling [44–47].

Therefore, with p_{tot} extracted and $\langle\hat{O}\rangle$ measured the only unknown quantity in Eq. (5) is the desired error-free observable $\text{Tr}[\hat{\text{O}}\rho_{\text{exact}}]$. Note, we assume that $\text{Tr}[\hat{\text{O}}]$ can be calculated which for most practical cases should be the case, e.g., see our application examples below.

Putting all steps together, we finally obtain our general error mitigation protocol:

(1) Prepare the quantum state of interest by running a quantum circuit and measure $\text{Tr}(\rho^2)$, e.g., via randomized measurements [36,41,42].

(2) Use the results to obtain values for p_{tot} via Eq. (6).

(3) Prepare the quantum state again and measure the desired observable $\langle\hat{O}\rangle$ [48].

(4) Use Eq. (5) with the measured value of p_{tot} to obtain the desired $\text{Tr}[\hat{\text{O}}\rho_{\text{exact}}]$.

An alternative approach to estimating p_{tot} is to consider specific observables whose expectation values are known. For example, consider the time dynamics of a system in which our quantum circuit approximates the time evolution operator $U(t) = \exp -iHt$ where we wish to measure $\langle O(t)\rangle$ for a range of times. We can tune the circuit such that $t * (E_{\text{max}}) = \epsilon << 1$ where E_{max} is the largest eigenvalue of the Hamiltonian (shifted so $E_{\text{min}} = 0$), so that our quantum circuit now approximates the identity operation. Assuming that $\langle O(t = 0)\rangle$ is known, we can use the measurements from the quantum device and Eq. (5) to obtain p_{tot}. Note, for infinite dimensional Hamiltonians with unbounded eigenvalues, the approximation is slightly more subtle, but does not apply to qubits. We show that, while this method is more efficient, it does not discriminate between coherent and incoherent errors in the purity.

Our protocol can be applied to essentially any quantum circuit and quantum simulation device. In the following, we choose a representative example from condensed matter physics as a first application. We showcase the effectiveness of our technique by presenting previously unobtainable results for confinement and entanglement dynamics in spin chains.

III. APPLICATION TO SPIN CHAIN CONFINEMENT

An ideal testing ground for NISQ devices is that of quench dynamics in spin-$\frac{1}{2}$ systems. A global quantum quench is a sudden change to the systems Hamiltonian, which induces nonequilibrium dynamics. Already one dimensional spin chains can show a wide variety of physical phenomena of interest, for example confinement of domain wall excitations [36,49,50], quantum many-body scars [51–55], or novel fracton excitations [56–58]. All of these show up in the time evolution which is challenging to simulate on classical computers as the Hilbert space grows exponentially 2^n with the number of spins n. As spin-$\frac{1}{2}$ systems directly map onto physical qubits, quantum computers are ideally suited for studying the rich physics of spin chains. Recently, first digital quantum simulation results have been reported [24,36,59–62] but to obtain results which are out of reach by classical simulations and to probe nontrivial quantum many body physics better error mitigation techniques are needed.

We concentrate on the one-dimensional TFIM with an additional longitudinal field given by the following Hamiltonian:

$$H = -J\left[\sum_i \sigma_i^z\sigma_{i+1}^z + h_x\sum_i \sigma_i^x + h_z\sum_i \sigma^z\right], \tag{7}$$

where J is the Ising exchange of nearest neighbor spins σ_i and $h_{x/z}$ are the relative strengths of the transverse and longitudinal fields respectively. For $h_z = 0$ the TFIM can be solved exactly via Jordan-Wigner transformation and its fermionic excitations are related to free domain wall motion. When turning on the longitudinal field, $h_z \neq 0$, a confining potential between these fermions is introduced. The attraction between fermions grows linearly with their separation, reminiscent of quark confinement in QCD. The result is the formation of "mesonic" bound states of domain wall excitations.

The confining potential between fermions induces nonergodic behavior [63], which manifests itself through persistent oscillations in the local magnetization, $\langle\sigma_i^\alpha\rangle$ ($\alpha \in \{x, y, z\}$) and a slowing down of the entanglement spreading.

A. Example 1: Measuring meson masses

The frequencies of the oscillating magnetization can be mapped directly to the energy of the domain wall bound states [50], which have a large overlap with chosen initial states. These so called *meson masses* are defined as the energy difference between the lowest excited states and the ground state.

Recent work using a trapped ion quantum simulator to simulate the long-range TFIM model showed how, by choosing a variety of initial states, the meson masses can be measured through the persistent oscillations of local magnetization [64]. Previous attempts to perform a similar measurement on a digital quantum computer have failed for the short ranged TFIM, Eq. (7), because the results are too noisy to resolve the smaller amplitude of oscillations [36]. As our main result, we show that our new error mitigation enables us to obtain the meson masses from an IBM Quantum device.

We are mainly interested in the time dependence of the local magnetization, which further simplifies with $\mathrm{Tr}[\sigma^\alpha] = 0$ in Eq. (5) to

$$\langle\sigma_i^\alpha\rangle = (1 - p_{\mathrm{tot}})\langle\sigma_i^\alpha\rangle_{\mathrm{exact}}. \tag{8}$$

The time dependence can be calculated by applying a quantum circuit from a Trotterization of the time evolution operator (for details of the implementation and quantum circuits see Refs. [24,36]). Increasing the number of trotter steps, N_t, leads to a deeper circuit and the ensuing increase in errors results in a peculiar dampening of the magnetization dynamics which can be removed via our error mitigation. In Fig. 2 we display the results of the local magnetization dynamics. Our mitigation technique not only allows us to measure the main oscillation frequency on the IBM device but in fact to do so with quantitative agreement with the analytical results (the latter is explained in Ref. [36]).

We note that an additional simplification can be used for the local magnetization for added efficiency—no additional measurement of $\mathrm{Tr}[\rho^2]$ was required because the result of $\langle\sigma^z\rangle$ is known at $tJ = 0$ and thus p_{tot} can be inferred from the corresponding measurement on the IBM device after running the time evolution circuit for $tJ \approx 0$. This big simplification avoids the costly randomized measurement scheme and should be generally applicable for observables whose value is known at $tJ = 0$. However, as this does not distinguish correlated noise from the uncorrelated noise assumed in our ansatz, it is possible for over-estimations in the mitigation to occur, resulting in nonphysical results. An example of this is seen in Fig. 2 at time $tJ = 0.1$ in which the local magnetization is measured to be greater than unity.

We have obtained a range of results with different number of trotter steps. Under the assumption that $(1 - p_{\mathrm{tot}})$ scales as $(1 - p_T)^{N_T}$, where p_T is the error in one trotter step, we can extrapolate the results back to the error-free case, see green data points in Fig. 2. We are then in a position to suppress the noise to a level which enables us to extract different meson masses on the IBM device by a basic fit of the main oscillation frequency. In Fig. 3 we show the data for the first three masses obtainable by starting from different initial states, see insets. Here, 7 spins are mapped onto 5 qubits resulting in a circuit with $5N_T + 5$ single qubit gates and $8N_T$ CNOT gates with $N_T = 5, 6$. Remarkably, we find quantitative agreement between the mitigated results and the theoretical predictions for the scaling of the meson masses with the transverse and longitudinal fields [36].

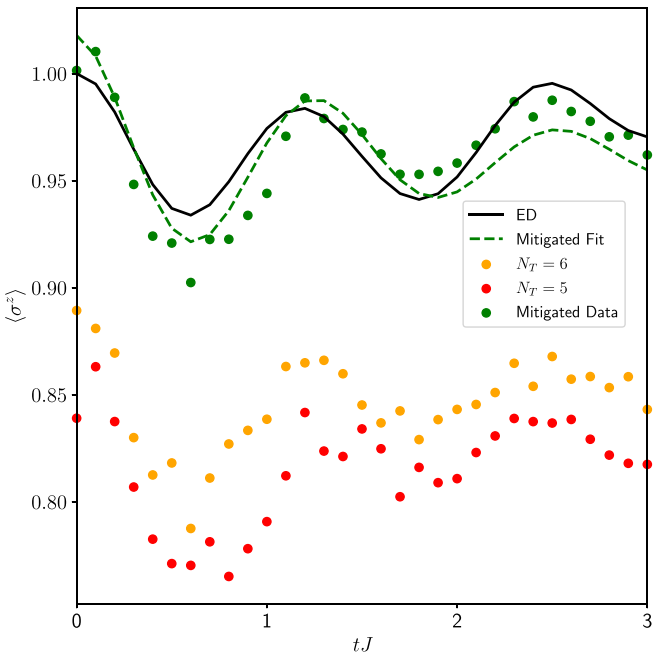

FIG. 2. Results from the IBM device *ibmq_toronto* [65] before and after mitigation. Quench dynamics of local magnetization from Trotterized time evolution of the TFIM with longitudinal field before and after error mitigation. Here, $J = 1$, $h_x = 0.5$, $h_x = 0.75$, and $n = 7$. Data is shown for N_t, the number of trotter steps $N_t = 5, 6$. Results go from qualitative agreement to quantitative agreement. After fitting a cosine function (dashed green) to the mitigated data (green dots) the dominant frequency is clearly captured by the IBM device. Note, more details of the circuit composition of the evolution operator can be found in Ref. [36].

B. Example 2: Entanglement Spreading

As a second example we study the suppression of half chain entanglement entropy spreading after the spin chain quench. For $h_z = 0$ the entanglement entropy is expected to increase linearly from the ballistic spreading of free fermionic excitations [66]. However, with a nonzero longitudinal field this growth is suppressed in a characteristic fashion due to confinement [49]. To observe this we have implemented the randomized measurement protocol of Ref. [42] on the IBM device for measuring the second-order Réyni entanglement entropy. In Ref. [36] two of us obtained qualitative agreement for entanglement dynamics of six spins compared to an exact diagonalization (ED) calculation, but for a quantitative agreement a large shift of the results was needed.

By using the ansatz in Eq. (4) we can see that the effect of global depolarizing errors on measurements of $\mathrm{Tr}[\rho_{\mathrm{A}}^2]$, where

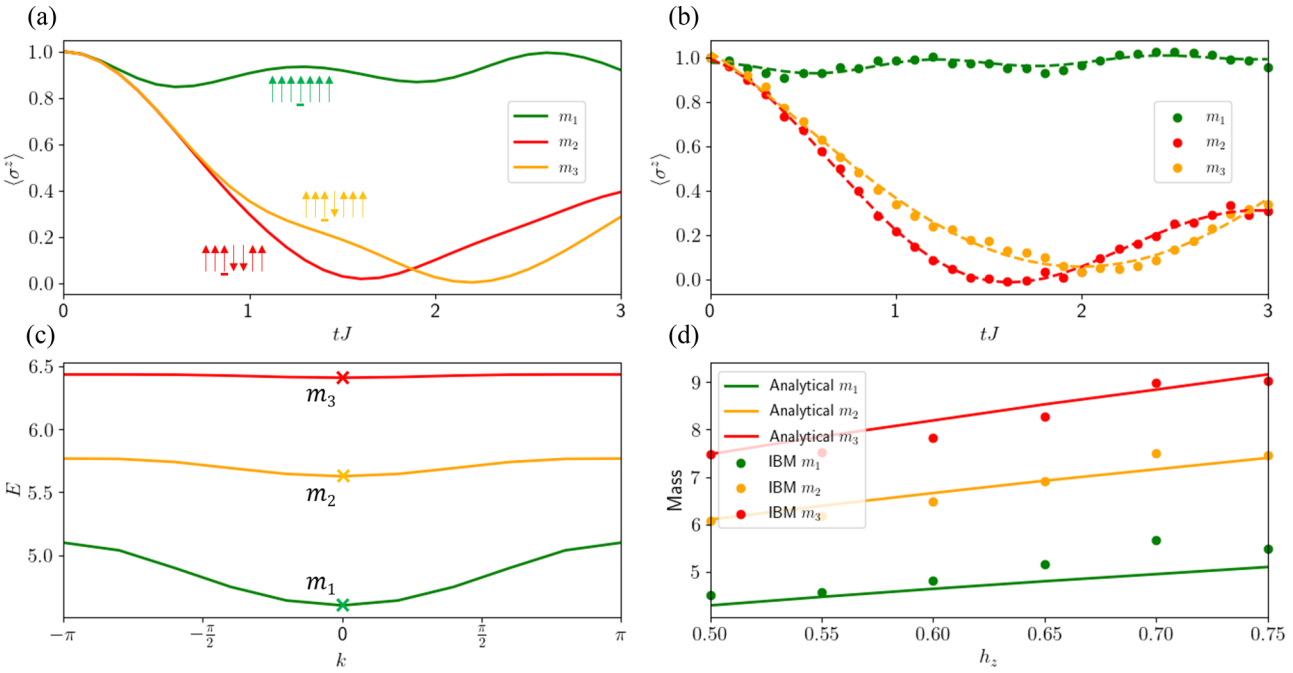

FIG. 3. Results from the IBM device *ibmq_toronto* [65] of meson masses. (a), (b) The quench dynamics of the z-axis local magnetization is shown for different initial states. Here, $J = 1$, $h_x = 0.75$, $h_x = 0.75$ and $n = 7$. (a) Results calculated via exact diagonalizion. (b) Mitigated results from the IBM device. Here, clear dominant oscillations are extracted that quantitatively agree with the analytically derived values. (c) An illustration of how the masses are extracted from the analytically derived energy levels [36]. (d) A comparison of the masses obtained from the IBM device and the analytically derived values for varying h_z showing this quantitative agreement. Note, more details of the circuit composition of the evolution operator can be found in Ref. [36]

A is a subsystem in consideration, is

$$\mathrm{Tr}\left[\rho_{\mathrm{A}}^2\right] = (1-\mathrm{p_{tot}})^2\mathrm{Tr}\left[\rho_{\mathrm{A,exact}}^2\right] + \frac{\mathrm{p_{tot}}(1-\mathrm{p_{tot}})}{2^{\mathrm{n_A}-1}} + \frac{\mathrm{p_{tot}}^2}{2^{\mathrm{n_A}}}. \tag{9}$$

If p_{tot} is known, then $\mathrm{Tr}[\rho_{\mathrm{A,exact}}^2]$ can be extracted and the second-order Rényi entropy measurement is calculated via

$$S^{(2)}(\rho_{\mathrm{exact}}) = -\log_2\left(\mathrm{Tr}[\rho_{\mathrm{A,exact}}^2]\right). \tag{10}$$

Figure 1 shows how this mitigation protocol eliminates the error in the second-order Rényi entropy results. With our error mitigation protocol and Eq. (9) we now obtain quantitative agreement with ED results for six spins and can account for the large shift of the results.

IV. APPLICATIONS TO MORE GENERAL EXAMPLES

To demonstrate that our method works more generally, we simulate example tasks of measuring the expectation value of different operators. We choose a layered, brickwork circuit consisting of a layer of single qubit rotations followed by a layer of entangling CNOTS—the same circuit structure as for Trotterized evolution [38]. However, instead of time parameterized Trotter evolution, we simply choose random single qubit angles, corresponding to different states, and therefore different expectation values.

To obtain a larger amount of data to support our mitigation technique, we numerically simulate the layered circuits with noisy gates. Qiskit's circuit simulator allows one to simulate arbitrary gate-based noise models by specifying independent Kraus operators for each single- and two-qubit gates. Using this noisy simulator, we can directly test how gate-level nondepolarizing errors can result in an effective global circuit-level depolarizing error, and how well our mitigation technique works in the presence of local nondepolarizing errors. To simulate a realistic noise model, we take the Kraus operators directly from the *ibmq_santiago* backend [67]. This error model goes beyond the single gate depolarizing assumption, by including (asymmetric) thermal relaxation.

To test local, nonlocal, single, and many Pauli-string operators, we have chosen the following operators: single Z operator (local, single term), TFIM Hamiltonian (local, many terms), Random Pauli string (nonlocal, single term), and the molecular Hamiltonian of a H_4 (nonlocal, many terms). Here "many terms" refers to the number of noncommuting Pauli strings that must be measured to construct the expectation value, and locality refers to only containing single and two-qubit Pauli strings. Note the four hydrogen Hamiltonian [38] is chosen as a simple molecular test case with a large Hilbert space, and where we can ignore complications from freezing out orbitals.

Figure 4 shows unmitigated and mitigated expectation values for each operator, and clearly demonstrates the added value of purity measurements [38]. For expectation value mitigation (i.e., using a single expectation value to calibrate p_{tot}), a single extra circuit is needed. For trace mitigation [using Eq. (9) to calibrate p_{tot}] uses 500 extra circuits to find p_{tot}; these are split into five groups to reduce the bias. Once p_{tot} is calibrated for a given circuit depth, this single value is used for error mitigation of the same circuit structure, but for different single qubit parameter angles.

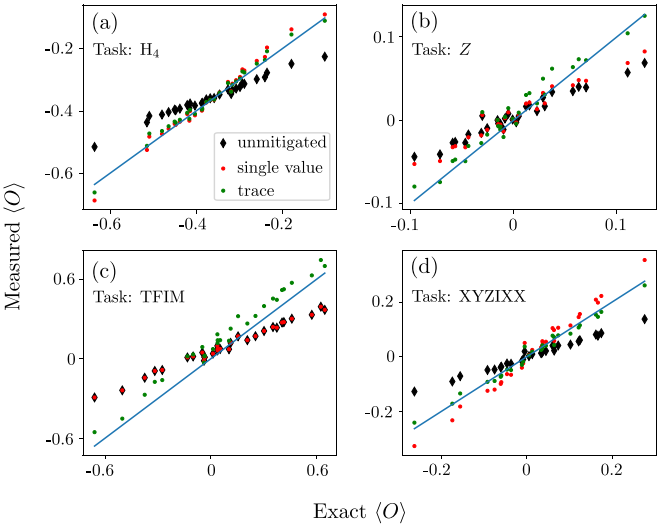

FIG. 4. Error mitigation simulations with nondepolarizing errors. Unmitigated (black diamonds), trace mitigated (green circles), and single operator mitigated (red circles) expectation values for different operators, with the solid blue line showing perfect mitigation. The numerical simulation uses the general error model taken from *ibmq_santiago*. Expectation values are evaluated with respect to parameterized brick-like circuits with (CNOT) depth 18, and thirty random parameter points per plot. Operators are (a) Hamiltonian of four linear-equidistant hydrogen atoms (6 qubits), (b) single Z Pauli term (8 qubits), (c) TFIM Hamiltonian (6 qubits), and (d) single $XYZIXX$ string (6 qubits). These operators are chosen to span local/global Pauli strings, and contain single/many noncommuting decompositions.

As the main results we find that our *global* depolarizing assumption is an effective error channel for the whole circuit, and, crucially, it does not require each single- and two-qubit errors to be themselves purely depolarizing.

V. DISCUSSION

In this work we have proposed an error mitigation technique which is simple to implement but which retains the mathematical rigour of more complicated techniques. Our protocol is directly applicable to any quantum simulation whose measurements are basic expectation values, as exemplified by our results for the time evolution of the local magnetization in spin chain dynamics. Though our error mitigation method may not replace full state tomography, we expect it to be useful in measuring more complicated quantities beyond simple observables, as corroborated by our results for the entanglement entropy. An interesting avenue of future research will be an application to variational quantum eigensolver (VQE) problems [68] and other quantum circuits.

The computational overhead of implementing our protocol is dominated by the cost of evaluating $\mathrm{Tr}(\rho^2)$ on the quantum device. The number of corresponding measurements is $N_u N_m$ where N_u is the number of randomized unitaries and N_m is the number of random measurements. Within the randomized scheme of Ref. [41] it grows exponentially with the system size [42], which poses a potential problem for large quantum computers but is easily feasible for currently available NISQ devices. Also, in some cases the costly randomized measurement scheme can be avoided entirely, i.e., in our benchmark example of spin chain dynamics a single measurement of a local observable whose exact value is known was sufficient. This should be true generally for quantum circuits which can be tuned to be close to the identity. However, this scalable simplification for obtaining p_{tot} potentially faces the problem that it includes correlated errors which makes the randomized measurements preferable as long as it is feasible.

The fact that our basic assumption of global depolarizing errors leads to such large improvements in results is in itself remarkable. The basic conclusion is that the total error on the IBM device is close to a global depolarizing error at least for our choice of problems. We note our error ansatz, Eq. (4) is an approximation even for single qubit depolarizing errors, let alone the more complex channels that are no-doubt present in physical devices. Nevertheless, the ansatz works remarkably well for correcting physical errors of large/deep circuits and is a no-lose addition to quantum simulation protocols. We suggest this is because the depolarizing channel is a good approximation *per gate* in a many gate quantum circuit, even if this approximation breaks down for single layers of gates. Of course, our mitigation falls short of accounting for large coherent or correlated errors and it will be a worthwhile endeavour to think about a controlled extension of our basic ansatz Eq. (4) for the density matrix of a NISQ device. In particular, whether we can extend it to incorporate other aspects of error channels [34].

As an application of our error mitigation we have presented previously unobtainable quantitative results for confinement and entanglement dynamics of a quantum spin chain. We have been able to extract the first meson masses of confinement induced bound states and observed the corresponding halting of entanglement spreading. In that context, an ambitious next step would be to use the error mitigation to extend times that can be simulated on a quantum computer to probe the confinement induced slow-thermalization [50] or to see meson scattering events that have recently been predicted [69–71].

In general, we expect that our simple error mitigation enables us to exploit available NISQ devices for their applications with significantly reduced errors.

Note added: We recently became aware of a complementary manuscript that not only builds on the mitigation protocol presented in our work but also favorably compares it to other established error mitigation techniques [72].

ACKNOWLEDGMENTS

We are grateful for discussions with Hongzheng Zhao, Adam Smith, and Peter Haynes. We acknowledge the Samsung Advanced Institute of Technology Global Research Partnership, travel support via the Imperial-TUM flagship cluster, and the use of IBM Quantum services for this work. The views expressed are those of the authors and do not reflect the official policy or position of IBM or the IBM Quantum team. This work is also supported by the UK Hub in Quantum Computing and Simulation, part of the UK National Quantum Technologies Programme with funding from UKRI EPSRC Grant No. EP/T001062/1.

[1] J. Preskill, Quantum **2**, 79 (2018).

[2] S. Boixo, S. V. Isakov, V. N. Smelyanskiy, R. Babbush, N. Ding, Z. Jiang, M. J. Bremner, J. M. Martinis, and H. Neven, Nat. Phys. **14**, 595 (2018).

[3] F. Arute, K. Arya, R. Babbush, D. Bacon, J. C. Bardin, R. Barends, R. Biswas, S. Boixo, F. G. Brandao, D. A. Buell *et al.*, Nature (London) **574**, 505 (2019).

[4] A. M. Steane, Phys. Rev. Lett. **77**, 793 (1996).

[5] P. W. Shor, Phys. Rev. A **52**, R2493(R) (1995).

[6] *ibmq_paris* v1.6.23, IBM Quantum Team. Retrieved from https://quantum-computing.ibm.com (2020).

[7] M. D. Sajid Anis *et al.*, Qiskit: An open-source framework for quantum computing (2021), doi:10.5281/zenodo.2573505.

[8] M. S. Jattana, F. Jin, H. De Raedt, and K. Michielsen, Quant. Info. Proc. **19**, 414 (2020).

[9] F. B. Maciejewski, Z. Zimborás, and M. Oszmaniec, Quantum **4**, 257 (2020).

[10] S. Bravyi, S. Sheldon, A. Kandala, D. C. Mckay, and J. M. Gambetta, Phys. Rev. A **103**, 042605 (2021).

[11] Y. Chen, M. Farahzad, S. Yoo, and T.-C. Wei, Phys. Rev. A **100**, 052315 (2019).

[12] J. R. McClean, Z. Jiang, N. C. Rubin, R. Babbush, and H. Neven, Nat. Commun. **11**, 636 (2020).

[13] X. Bonet-Monroig, R. Sagastizabal, M. Singh, and T. E. O'Brien, Phys. Rev. A **98**, 062339 (2018).

[14] R. Sagastizabal, X. Bonet-Monroig, M. Singh, M. A. Rol, C. C. Bultink, X. Fu, C. H. Price, V. P. Ostroukh, N. Muthusubramanian, A. Bruno, M. Beekman, N. Haider, T. E. OBrien, L. Di Carlo, Phys. Rev. A **100**, 010302(R) (2019).

[15] M. C. Tran, Y. Su, D. Carney, and J. M. Taylor, PRX Quantum **2**, 010323 (2021).

[16] W. J. Huggins, J. McClean, N. Rubin, Z. Jiang, N. Wiebe, K. B. Whaley, and R. Babbush, npj Quantum Inf **7**, 23 (2021).

[17] S. McArdle, X. Yuan, and S. Benjamin, Phys. Rev. Lett. **122**, 180501 (2019).

[18] E. F. Dumitrescu, A. J. McCaskey, G. Hagen, G. R. Jansen, T. D. Morris, T. Papenbrock, R. C. Pooser, D. J. Dean, and P. Lougovski, Phys. Rev. Lett. **120**, 210501 (2018).

[19] J. R. McClean, M. E. Kimchi-Schwartz, J. Carter, and W. A. de Jong, Phys. Rev. A **95**, 042308 (2017).

[20] J. I. Colless, V. V. Ramasesh, D. Dahlen, M. S. Blok, M. E. Kimchi-Schwartz, J. R. McClean, J. Carter, W. A. de Jong, and I. Siddiqi, Phys. Rev. X **8**, 011021 (2018).

[21] A. Kandala, K. Temme, A. D. Córcoles, A. Mezzacapo, J. M. Chow, and J. M. Gambetta, Nature (London) **567**, 491 (2019).

[22] M. Otten and S. K. Gray, npj Quantum Inf. **5**, 11 (2019).

[23] M. Otten and S. K. Gray, Phys. Rev. A **99**, 012338 (2019).

[24] A. Smith, M. S. Kim, F. Pollmann, and J. Knolle, npj Quantum Inf. **5**, 106 (2019).

[25] A. Strikis, D. Qin, Y. Chen, S. C. Benjamin, and Y. Li, arXiv:2005.07601.

[26] A. Zlokapa and A. Gheorghiu, arXiv:2005.10811.

[27] P. Czarnik, A. Arrasmith, P. J. Coles, and L. Cincio, arXiv:2005.10189.

[28] A. Lowe, M. H. Gordon, P. Czarnik, A. Arrasmith, P. J. Coles, and L. Cincio, Phys. Rev. Research, **3**, 033098 (2021).

[29] Y. Li and S. C. Benjamin, Phys. Rev. X **7**, 021050 (2017).

[30] S. Endo, S. C. Benjamin, and Y. Li, Phys. Rev. X **8**, 031027 (2018).

[31] K. Temme, S. Bravyi, and J. M. Gambetta, Phys. Rev. Lett. **119**, 180509 (2017).

[32] E. Gustafson, Y. Meurice, and J. Unmuth-Yockey, Phys. Rev. D **99**, 094503 (2019).

[33] T. Giurgica-Tiron, Y. Hindy, R. LaRose, A. Mari, and W. J. Zeng, *2020 IEEE International Conference on Quantum Computing and Engineering (QCE)* (IEEE, New York, 2020), pp. 306–316.

[34] Z. Cai, npj Quantum Inf. **7**, 80 (2021).

[35] A. He, B. Nachman, W. A. de Jong, and C. W. Bauer, Phys. Rev. A **102**, 012426 (2020).

[36] J. Vovrosh and J. Knolle, Sci. Rep. **11**, 11577 (2021).

[37] M. A. Nielsen and I. Chuang, *Quantum Computation and Quantum Information* (American Association of Physics Teachers, 2002).

[38] See Supplemental Material at http://link.aps.org/supplemental/10.1103/PhysRevE.104.035309 for a further justification of the linear ansatz, details on the meson mass extraction, and more information on the simulations presented in this work. This includes the additional Refs. [73,74].

[39] B. Vermersch, A. Elben, M. Dalmonte, J. I. Cirac, and P. Zoller, Phys. Rev. A **97**, 023604 (2018).

[40] S. J. van Enk and C. W. J. Beenakker, Phys. Rev. Lett. **108**, 110503 (2012).

[41] A. Elben, B. Vermersch, M. Dalmonte, J. I. Cirac, and P. Zoller, Phys. Rev. Lett. **120**, 050406 (2018).

[42] T. Brydges, A. Elben, P. Jurcevic, B. Vermersch, C. Maier, B. P. Lanyon, P. Zoller, R. Blatt, and C. F. Roos, Science **364**, 260 (2019).

[43] A. Elben, B. Vermersch, R. van Bijnen, C. Kokail, T. Brydges, C. Maier, M. K. Joshi, R. Blatt, C. F. Roos, and P. Zoller, Phys. Rev. Lett. **124**, 010504 (2020).

[44] C. H. Bennett, D. P. DiVincenzo, J. A. Smolin, and W. K. Wootters, Phys. Rev. A **54**, 3824 (1996).

[45] C. H. Bennett, G. Brassard, S. Popescu, B. Schumacher, J. A. Smolin, and W. K. Wootters, Phys. Rev. Lett. **76**, 722 (1996).

[46] E. Knill, D. Leibfried, R. Reichle, J. Britton, R. B. Blakestad, J. D. Jost, C. Langer, R. Ozeri, S. Seidelin, and D. J. Wineland, Phys. Rev. A **77**, 012307 (2008).

[47] J. Emerson, M. Silva, O. Moussa, C. Ryan, M. Laforest, J. Baugh, D. G. Cory, and R. Laflamme, Science **317**, 1893 (2007).

[48] As errors on the quantum devices can vary over time (see Ref. [24]), the determination of p_{tot} has to be recalibrated accordingly.

[49] M. Kormos, M. Collura, G. Takács, and P. Calabrese, Nat. Phys. **13**, 246 (2017).

[50] F. Liu, R. Lundgren, P. Titum, G. Pagano, J. Zhang, C. Monroe, and A. V. Gorshkov, Phys. Rev. Lett. **122**, 150601 (2019).

[51] C. J. Turner, A. A. Michailidis, D. A. Abanin, M. Serbyn, and Z. Papić, Nat. Phys. **14**, 745 (2018).

[52] S. Moudgalya, S. Rachel, B. A. Bernevig, and N. Regnault, Phys. Rev. B **98**, 235155 (2018).

[53] W. W. Ho, S. Choi, H. Pichler, and M. D. Lukin, Phys. Rev. Lett. **122**, 040603 (2019).

[54] D. K. Mark, C.-J. Lin, and O. I. Motrunich, Phys. Rev. B **101**, 195131 (2020).

[55] N. Shibata, N. Yoshioka, and H. Katsura, Phys. Rev. Lett. **124**, 180604 (2020).

[56] R. M. Nandkishore and M. Hermele, Annu. Rev. Condens. Matter Phys. **10**, 295 (2019).
[57] S. Pai and M. Pretko, Phys. Rev. Res. **2**, 013094 (2020).
[58] P. Sala, T. Rakovszky, R. Verresen, M. Knap, and F. Pollmann, Phys. Rev. X **10**, 011047 (2020).
[59] A. Cervera-Lierta, Quantum **2**, 114 (2018).
[60] A. Zhukov, S. Remizov, W. Pogosov, and Y. E. Lozovik, Quant. Info. Proc. **17**, 223 (2018).
[61] A. Francis, J. Freericks, and A. Kemper, Phys. Rev. B **101**, 014411 (2020).
[62] A. Smith, B. Jobst, A. G. Green, and F. Pollmann, arXiv:1910.05351.
[63] A. J. A. James, R. M. Konik, and N. J. Robinson, Phys. Rev. Lett. **122**, 130603 (2019).
[64] W. L. Tan, P. Becker, F. Liu, G. Pagano, K. S. Collins, A. De, L. Feng, H. B. Kaplan, A. Kyprianidis, R. Lundgren *et al.*, Nat. Phys. **17**, 742 (2021).
[65] *ibmq_toronto* v1.1.6, IBM Quantum Team. Retrieved from https://quantum-computing.ibm.com (2020).
[66] M. Fagotti and P. Calabrese, Phys. Rev. A **78**, 010306(R) (2008).
[67] *ibmq_santiago* v1.3.19, IBM Quantum Team. Retrieved from https://quantum-computing.ibm.com (2021).
[68] A. Kandala, A. Mezzacapo, K. Temme, M. Takita, M. Brink, J. M. Chow, and J. M. Gambetta, Nature (London) **549**, 242 (2017).
[69] F. M. Surace and A. Lerose, New J. Phys. **23**, 062001 (2021).
[70] P. I. Karpov, G.-Y. Zhu, M. P. Heller, and M. Heyl1, arXiv:2011.11624.
[71] A. Milsted, J. Liu, J. Preskill, and G. Vidal, arXiv:2012.07243.
[72] A. Sopena, M. H. Gordon, G. Sierra, and E. López, Quantum Sci. Technol. **6**, 045003 (2021).
[73] J. R. McClean, N. C. Rubin, K. J. Sung, I. D. Kivlichan, X. Bonet-Monroig, Y. Cao, C. Dai, E. S. Fried, C. Gidney, B. Gimby, P. Gokhale, T. Häner, T. Hardikar, V. Havlíček, O. Higgott, C. Huang, J. Izaac, Z. Jiang, X. Liu, S. McArdle *et al.*, Quantum Sci. Technol. **5**, 034014 (2020).
[74] S. Bravyi, J. M. Gambetta, A. Mezzacapo, and K. Temme, arXiv:1701.08213.